

Predictive evolution of dusty plasma instabilities

H. Tawidian, T. Lecas, M. Mikikian

GREMI, UMR7344 CNRS/Université d'Orléans, 14 rue d'Issoudun, BP6744, 45067 Orléans Cedex 2, FRANCE

The occurrence of low frequency instabilities [1, 2] in a plasma can be due to the presence of a high density of grown dust particles. In this contribution, these instabilities are characterized by analyzing the discharge current. The measurements show the existence of successive phases marked by distinct frequency evolutions. The main instability characteristics are determined as a function of the gas pressure [3]. The instability appearance time is the first parameter that can be easily measured during an experiment. It is shown that it can be used to predict the instability evolution and its other main characteristics.

The experiments are performed in the PKE-Nefedov [4] reactor where the plasma is created by a capacitively coupled radio-frequency (13.56 MHz) discharge with a typical power of about 3 W. The reactor is constituted of two parallel electrodes separated by 3 cm and with a diameter of 4.2 cm surrounded by guard rings. Dust particles are grown in the plasma by sputtering previously injected micrometer size dust particles made of polymer (melamine formaldehyde) and lying on the electrode [5]. Krypton is used as the sputtering gas with a typical pressure between 1.4 and 2.4 mbar. Once the plasma is switched on, the growth process starts. This growth is easily identified by measuring the temporal evolution of the amplitude (DC component) of the discharge current fundamental harmonic. Indeed, as dust particles are growing, they attach more and more free electrons. It results in the global decrease of the discharge current. After a few tens of seconds, dust particles strongly disturb the plasma equilibrium and dust particle growth instabilities (DPGI) start. During DPGI, the plasma is highly unstable and shows very complex structure and behavior [6, 7]. In order to study DPGI with a much higher resolution, we analyzed the AC component of the amplitude of the discharge current. This analysis provides useful information on the growth kinetics and on the instability evolution. In Fig. 1a, the AC part of the discharge current is recorded from the plasma ignition till its extinction at a pressure of 1.8 mbar. The plasma ignition is detected as a sharp peak 3 s after the recording start. The instability begins several tens of seconds after the plasma ignition and lasts about 2000 s. In order to bring to light the DPGI frequency evolution, the corresponding Fourier spectrogram is calculated (Fig. 1b). In order to emphasize small ordered domains, the spectrogram intensity has been normalized separately inside each 100 s range.

From these Figures, it clearly appears that the instability is characterized by a well defined

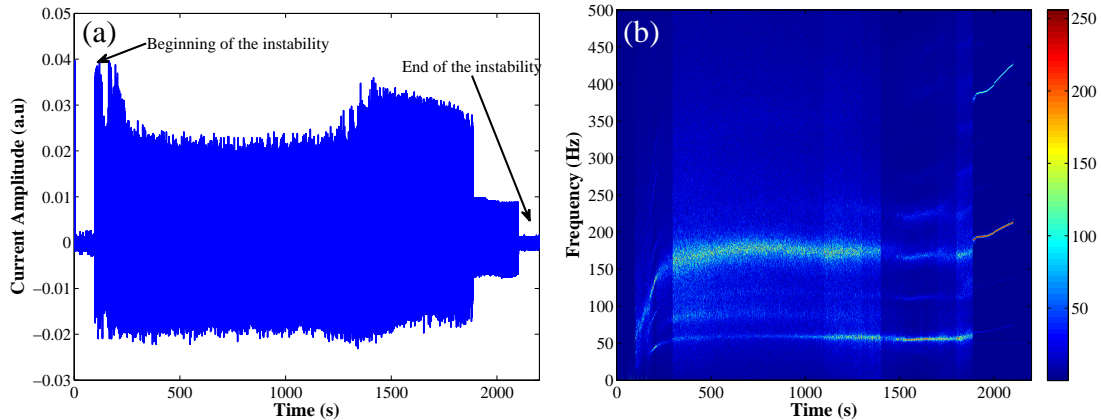


Figure 1: (a) Alternative part of the discharge current amplitude evidencing DPGI. (b) Fourier spectrogram of the electrical measurements and representing the frequency evolution during DPGI.

succession of phases. These phases can be either ordered with a smoothly evolving frequency or stochastic with fast and erratic frequency variations. In Fig. 1b, the stochastic phase clearly appears between 400 and 1300 s. These phases are also well identified in Fig. 1a where they are characterized by different instability amplitudes. In Fig. 1b, when several frequencies are detected simultaneously, the color code allows to identify the dominant frequency. Indeed, the electrical measurements show that the instability is constituted of well defined patterns with a varying number of peaks [8]. At the beginning of the instability, a fast increase of the frequency is observed until 400 s (Fig. 1b). During this period, the instability alternates between ordered and more stochastic phases. Then, a long stochastic phase starts at 400 s up to 1300 s. The frequency fluctuates around 170 Hz quickly and erratically but stays within a rather small value range. During this period, the envelop amplitude of the electrical signal stays roughly at the same height (Fig. 1a) and the most highlighted frequency (Fig. 1b) corresponds to the frequency between consecutive peaks. During this phase no specific pattern can be determined due to the stochastic evolution. Then, the frequency drops to a lower level (55 Hz) at around 1300 s. This drop appears as an increase of the signal amplitude in Fig. 1a, and a pattern with two peaks can be observed during this phase. However in this case, the dominant frequency is the main pattern frequency. Finally, the instability ends with an ordered phase characterized by a high frequency (≈ 200 Hz in Fig. 1b) and a small amplitude (Fig. 1a).

We have identified different phases and a complex evolution of the main frequency. In order to better understand the instability behavior, its modification as a function of the pressure is now investigated. For each pressure, several experiments are performed in order to obtain statistical measurements and estimate the related error bars. In Fig. 2a, the appearance time and the total duration of DPGI are presented as a function of the pressure. At 1.4 mbar, the instability appears

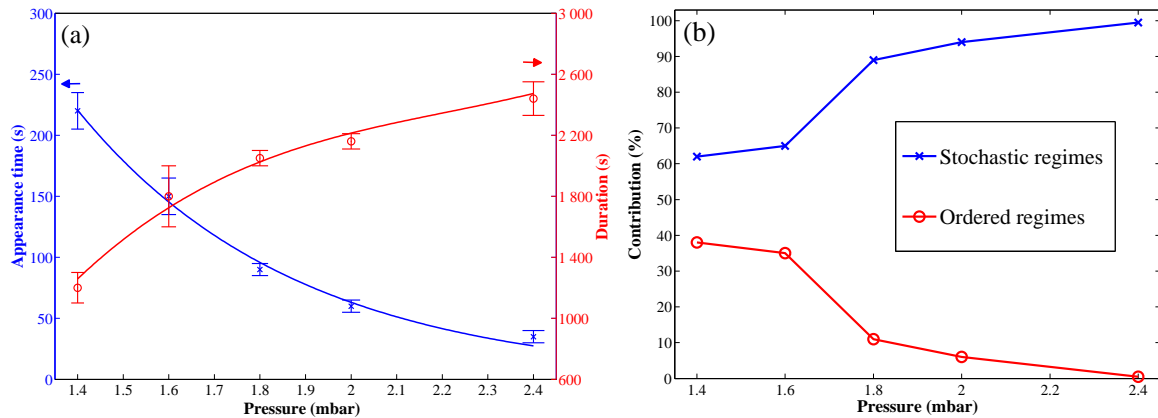


Figure 2: (a) Appearance time (\times) and total duration (\circ) of DPGI as a function of gas pressure. (b) Contribution of the ordered (\circ) and stochastic (\times) regimes as a function of the pressure.

around 220 s after the plasma ignition. Increasing the pressure results in a continuous decrease of the appearance time that can be easily fitted by a decreasing exponential function. At 2.4 mbar, DPGI occur relatively quickly after the plasma ignition (35 s). It means that the necessary conditions to trigger DPGI are obtained faster at high pressure. It is consistent with the observation that higher pressures result in the growth of a higher dust density (and thus smaller dust sizes). These conditions seem to be more favorable to trigger DPGI than situations with a lower density of bigger dust particles obtained at low pressures. Concerning the instability duration, it increases with the pressure from 1200 s at 1.4 mbar up to 2400 s at 2.4 mbar. The duration trend can be also fitted by an exponential function in the form $a - b \cdot \exp(-c \cdot P)$. It means that at high pressure, the amount of dust particles is high enough to maintain a longer instability. From these behaviors, it can be deduced that the higher the pressure, the shorter the appearance time and the longer the duration of the instability. Thus, a high dust particle density induced well developed DPGI.

As we showed that DPGI consist of a succession of phases, the relative contributions of the ordered and stochastic phases have been estimated (Fig. 2b). The durations of all the stochastic phases occurring during a DPGI sequence have been summed up. The same procedure has been used for the ordered regimes. At 1.4 mbar, the two types of phases have roughly the same duration, whereas the stochastic phases become dominant as the pressure is increased. At 2.4 mbar, the ordered phases are almost absent, and DPGI are mainly stochastic during their whole duration. It means that when the dust particle density is huge (and thus the dust particle size is small), the instability cannot enter in an ordered regime. The disturbance induced by the dust particles is too strong to allow the instability to have an ordered oscillating behavior.

Finally, the possibility to predict the instability evolution is presented. Relations between the instability characteristics can be emphasized. During an experiment, the first parameter that

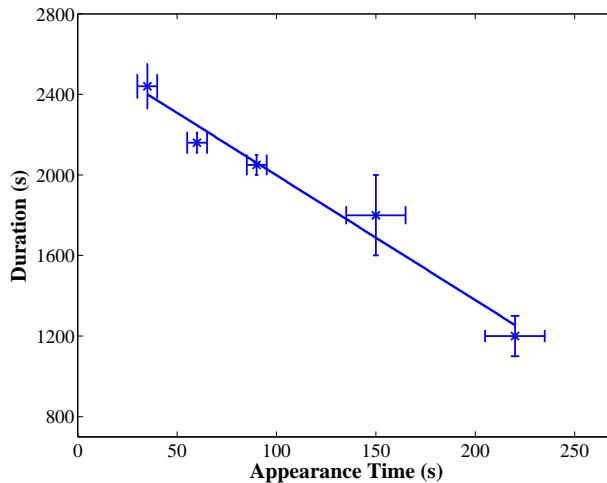


Figure 3: Duration of the entire instability as a function of the appearance time.

can be easily measured is the instability appearance time. We show that the knowledge of this parameter can provide information on the instability evolution. In Fig. 3, the instability duration is plotted as a function of the appearance time.

For future work, in order to have an access to dust particle size and a better correlation with DPGI evolution, in-situ diagnostics like ellipsometry will be performed.

Acknowledgments

The PKE-Nefedov chamber has been made available by the Max-Planck-Institute for Extraterrestrial Physics, Germany, under the funding of DLR/BMBF under Grant No. 50WM9852.

This work was supported by the French National Research Agency (ANR), project INDIGO n° ANR-11-JS09-010-01.

References

- [1] D. Samsonov and J. Goree, Phys. Rev. E **59**, 1047 (1999)
- [2] M. Mikikian, M. Cavarroc, L. Couëdel, and L. Boufendi, Phys. Plasmas **13**, 092103 (2006)
- [3] H. Tawidian, T. Lecas, and M. Mikikian, Submitted (2013)
- [4] A. P. Nefedov, G. E. Morfill, V. E. Fortov, H. M. Thomas, H. Rothermel, T. Hagl, A. Ivlev, M. Zuzic, B. A. Klumov, A. M. Lipaev, V. I. Molotkov, O. F. Petrov, Y. P. Gidzenko, S. K. Krikalev, W. Shepherd, A. I. Ivanov, M. Roth, H. Binnenbrück, J. Goree, and Y. P. Semenov, New J. Phys. **5**, 33 (2003)
- [5] M. Mikikian, L. Boufendi, A. Bouchoule, H. M. Thomas, G. E. Morfill, A. P. Nefedov, V. E. Fortov, and the PKE-Nefedov Team, New J. Phys. **5**, 19 (2003)
- [6] H. Tawidian, M. Mikikian, L. Couëdel, and T. Lecas, Eur. Phys. J. Appl. Phys. **56**, 24018 (2011)
- [7] M. Mikikian, H. Tawidian, and T. Lecas, Phys. Rev. Lett. **109**, 254007 (2012)
- [8] H. Tawidian, T. Lecas, and M. Mikikian, IEEE Trans. Plasma Sci. **41**, 754 (2013)